Atmospheric Environment 42 (2008) 6655–6669

Contents lists available at ScienceDirect

Atmospheric Environment

journal homepage: www.elsevier.com/locate/atmosenv

Semi-continuous measurement of $PM_{2.5}$ ionic composition at several rural locations in the United States

Taehyoung Lee [a], Xiao-Ying Yu [a,1], Sonia M. Kreidenweis [a], William C. Malm [a,b], Jeffrey L. Collett [a,b,*]

[a] Atmospheric Science Department, Colorado State University, Fort Collins, CO, USA
[b] National Park Service, Cooperative Institute for Research in the Atmosphere, Colorado State University, Fort Collins, CO, USA

ARTICLE INFO

Article history:
Received 4 October 2007
Received in revised form 2 April 2008
Accepted 8 April 2008

Keywords:
$PM_{2.5}$ composition
Particle-Into-Liquid-Sampler
Continuous measurements
Temporal variability

ABSTRACT

To improve understanding of the nature and variability of the ionic fraction of atmospheric fine aerosol particles in non-urban environments, one to two month measurement campaigns were conducted at several rural locations in the United States. Study sites included Yosemite National Park (NP) (July–September 2002), Bondville, Illinois (February 2003), San Gorgonio Wilderness Area, California (April and July 2003), Grand Canyon National Park, Arizona (May 2003), Brigantine National Wildlife Refuge (NWR), New Jersey (November 2003), and Great Smoky Mountains National Park, Tennessee (July/August 2004). $PM_{2.5}$ ion composition was measured at 15 min intervals using a Particle-Into-Liquid-Sampler (PILS) coupled to two ion chromatographs. Comparisons of PILS measurements with parallel traditional 24 h denuder/filter-pack measurements reveal generally good agreement between the two techniques for major species, although PILS measurements of $PM_{2.5}$ NH_4^+ are biased low by approximately 4–20%. High time resolution PILS aerosol concentration measurements provide better estimates of the range of aerosol concentrations at the rural locations than the 24 h integrated filter data. Ratios of peak 15 min to 24 h nitrate concentrations, for example, ranged from 1.7 at Brigantine NWR to 7.0 at Great Smoky Mountains NP. A strong influence of diurnal upslope/downslope transport patterns was observed on aerosol concentrations at several locations, including Yosemite NP, San Gorgonio Wilderness Area, and Great Smoky Mountains NP, with peak concentrations typically occurring during afternoon upslope transport. High time resolution aerosol composition measurements also provide new insight into relationships between individual aerosol species and the influence of environmental conditions on aerosol composition. Observations at several locations revealed important information about mechanisms of particle nitrate formation. At Yosemite and Grand Canyon National Parks, for example, evidence was observed for reaction of nitric acid or its precursors with sea salt or soil dust. Observations from several sites also revealed the importance of aerosol acidity (Great Smoky Mountains NP, Bondville) and temperature/humidity (San Gorgonio) on fine particle ammonium nitrate formation.

1. Introduction

Atmospheric aerosol particles play important roles in biogeochemical cycles, influence Earth's radiative balance, contribute to visibility degradation, and adversely impact human health (Jacobson, 2001; Malm et al., 2004; Nel,

* Corresponding author. National Park Service, Cooperative Institute for Research in the Atmosphere, Colorado State University, Fort Collins, CO, USA.
E-mail address: collett@atmos.colostate.edu (J.L. Collett Jr.).
[1] Present address: Atmospheric Science & Global Change Division, Pacific Northwest National Laboratory, WA, USA.

1352-2310/$ – see front matter © 2008 Elsevier Ltd. All rights reserved.
doi:10.1016/j.atmosenv.2008.04.023

2005). In a typical polluted atmosphere, the presence of NH_3 (ammonia), H_2SO_4 (sulfuric acid), and HNO_3 (nitric acid) can lead to formation of particulate ammonium nitrate (NH_4NO_3) and/or various forms of ammoniated sulfate (Finlayson-Pitts and Pitts, 2000; Lee et al., 2004; Seinfeld and Pandis, 2006; Spurny, 2000). Ammonium nitrate and ammoniated sulfate are generally considered the predominant forms of nitrate and sulfate in the inorganic fraction in submicron particles (Adams et al., 1999; Allegrini et al., 1994; Cheng and Tanner, 2002; Lee et al., 2008; Malm et al., 1994). Ammonium nitrate formation is a reversible reaction dependent on temperature and relative humidity (Appel, 1993; Spicer, 1977; Stelson and Seinfeld, 1982a; Stelson and Seinfeld, 1982b). Relatively high humidities and low temperatures favor particulate ammonium nitrate formation. Limitations to ammonium nitrate formation are common in many environments because ammonia reacts preferentially with H_2SO_4 to form ammonium sulfate ($[NH_4]_2SO_4$), letovicite ($[NH_4]_3H[SO_4]_2$), or ammonium bisulfate (NH_4HSO_4) (Lee et al., 1993; Lee et al., 2004). Ammonium nitrate formation is not thermodynamically favored until all sulfate present is fully neutralized (Seinfeld and Pandis, 2006). In ammonia-limited situations sea salt and soil dust particles can react with HNO_3 or its atmospheric precursors to form alternative forms of coarse particle nitrate including $NaNO_3$ (sodium nitrate) and $Ca(NO_3)_2$ (calcium nitrate) (Dentener et al., 1996; Goodman et al., 2000; Grassian, 2002; John et al., 1990; Laskin et al., 2005; Lee et al., 2004; Padgett and Bytnerowicz, 2001; Pakkanen, 1996; Pakkanen et al., 1996; Prospero and Savoie, 1989; Sullivan et al., 2006; Umann et al., 2005; Underwood et al., 2001; Zhuang et al., 1999a; Zhuang et al., 1999b).

Filter sampling techniques are often employed to measure particle composition. Filter measurements are often integrated over long time periods (e.g., 12–24 h or more), thereby limiting our knowledge of finer timescale variability in particle concentrations and our ability to relate observed particle composition to particular emissions, transport patterns or meteorological situations (Orsini et al., 2003; Sullivan et al., 2004; Weber et al., 2001; Wittig et al., 2004). Long sampling periods that include large variations in environmental conditions also can contribute to aerosol sampling artifacts, including losses of semi-volatile components from the filter medium (Appel, 1993; Appel and Tokiwa, 1981; Chow et al., 2005; Hering and Cass, 1999; Hering et al., 1988; Koutrakis et al., 1992; Pang et al., 2001; Yu et al., 2006).

In order to provide better insight into aerosol sources, atmospheric transport, and chemical reactions, a number of approaches have been developed recently to allow aerosol chemical composition measurements on much faster timescales (Buhr et al., 1995; Karlsson et al., 1997; Khlystov et al., 1995; Oms et al., 1996; Orsini et al., 2003; Simon and Dasgupta, 1993; Simon and Dasgupta, 1995; Slanina et al., 2001; Stolzenburg and Hering, 2000; Trebs et al., 2004; Weber et al., 2001; Zellweger et al., 1999). In this study, a PILS (Particle-Into-Liquid-Sampler) coupled to two ion chromatographs was used for high time resolution measurement of $PM_{2.5}$. Measurements were performed at several rural U.S. locations to enhance our understanding of the chemical characteristics of aerosol particles in non-urban locations and to provide new insight into the variability of particle concentrations and composition on sub-daily timescales. Results from these measurements demonstrate how air quality at many rural locations often depends on intermittent transport of polluted air masses from regions with higher emissions.

2. Methods

A series of intensive field experiments was designed and conducted to investigate semi-continuous aerosol particle concentrations and chemical composition at several rural sites. Study sites included Yosemite National Park, California (July–September 2002), Bondville, Illinois (February 2003), Brigantine National Seashore, New Jersey (November 2003), San Gorgonio Wilderness Area, California (April and July 2003), Grand Canyon National Park, Arizona (May 2003), and Great Smoky Mountains National Park, Tennessee (August 2004). All measurement sites were co-located with routine monitoring locations for the IMPROVE (Interagency Monitoring of PROtected Visual Environments) program. Fig. 1 summarizes site locations, altitudes, and measurement periods.

Measurements in Yosemite were made in summer as part of a study examining impacts of wildfires on regional haze (Engling et al., 2006; McMeeking et al., 2005a, b, 2006; Herckes et al., 2006). Several of the field campaigns were scheduled to examine locations and time periods when nitrate concentrations were near their annual peak, based on historical IMPROVE observations. Winter measurements at Bondville were intended to explore the importance of fine particle ammonium nitrate in the Midwest United States. Particle composition at Brigantine was studied in order to evaluate possible interactions between polluted and marine air masses. Two campaigns were conducted at San Gorgonio, a wilderness area site in the mountains downwind of the nitrate-rich Los Angeles Air basin. Spring and summer periods were included to investigate changes in particle composition with warming seasonal temperatures. The Grand Canyon site was selected to represent a visually important area of the southwestern U.S.; a spring study was conducted due to historically high seasonal nitrate contributions. Aerosol composition was studied in Great Smoky Mountains National Park in the SE U.S. in summer, a period of historically high acidic sulfate concentrations.

Semi-continuous measurements of $PM_{2.5}$ ion composition were made using a PILS system coupled to two ion chromatographs. The design and operation of the PILS have been previously described by several authors (Orsini et al., 2003; Sorooshian et al., 2006; Weber et al., 2003; Weber et al., 2001) and will be only briefly summarized here. The PILS nucleates aerosol particles to form water droplets by mixing a denuded aerosol stream with supersaturated steam. The nucleated droplets are collected into a flowing liquid stream by inertial impaction. The liquid stream, containing an internal LiBr standard to determine dilution by condensed water vapor, is split into two streams which are injected every 15 min to two ion chromatographs (Dionex, DX-500) for measurement of major

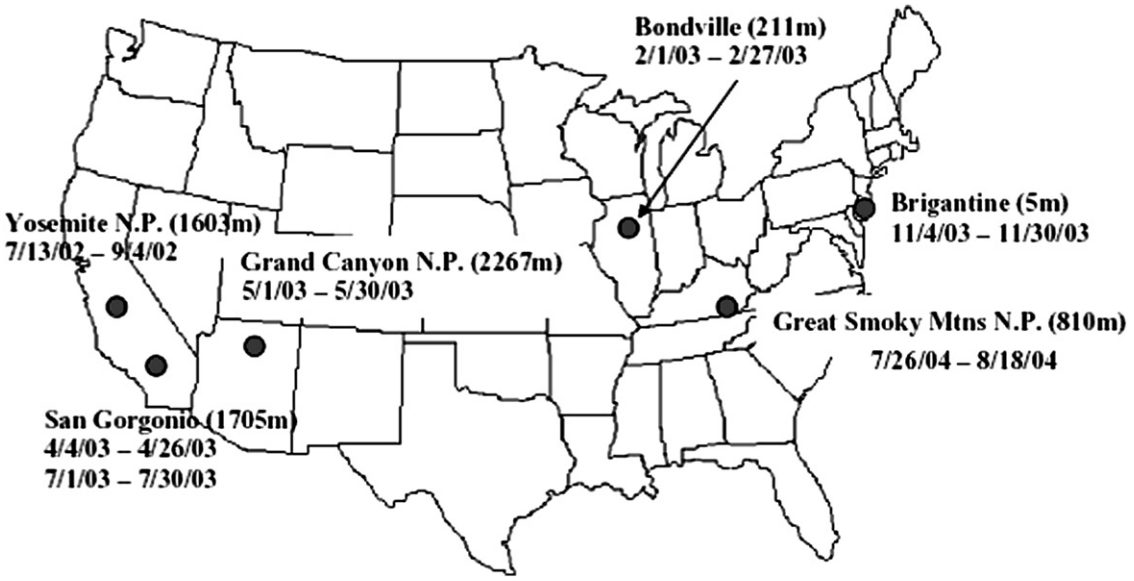

Fig. 1. Study site locations, altitudes, and measurement time periods.

inorganic ion (Cl^-, SO_4^{2-}, NO_3^-, Na^+, NH_4^+, K^+, Mg^{2+}, and Ca^{2+}) concentrations. Each IC system consisted of a 6-port valve injector fitted with a 200 μL sample loop, a pump (Dionex GP40 or IP20), Dionex CD20 conductivity detector, an analytical separation column, and a suppressor. The cation eluent was 20 mM MSA (methanesulfonic acid) at a flow rate of 1.0 mL min (Dionex CG12A/CS12A column and CSRS-ULTRA II suppressor). The anion system used a Dionex AS4A-SC/AG4A-SC column pair (1.8 mM Na_2CO_3/1.7 mM $NaHCO_3$ eluent) or a Dionex AS14A column (8 mM Na_2CO_3/7 mM $NaHCO_3$ eluent), depending on the campaign, with an ASRS-ULTRA II suppressor.

A $PM_{2.5}$ cyclone (16.7 LPM, URG-2000-30EH) and two URG annular denuders (URG-2000-30X242-3CSS) were used upstream of the PILS/IC. The first denuder was coated with Na_2CO_3 for removal of acidic gases and the second denuder was coated with phosphorous acid to remove basic gases. Denuders were exchanged every 5–6 days, immediately following PILS/IC calibration and blank checks. Approximately every 10 days the impaction surface inside the PILS was cleaned and the ion chromatograph recalibrated. A sample flow rate of 16.7 L min for the PILS/IC was controlled by a critical orifice with a vacuum regulator. An independent measurement of the flow rate was made every 5–6 days using a bubble flow meter (Sensidyne Gilibrator).

To determine the MDL (Minimum Detection Limit at the 95% confidence limit), blanks taken by sampling particle-free air, drawn through a HEPA capsule filter (12144, Pall Life Science) and into the PILS-IC system were used. The MDL values determined for major ion components (SO_4^{2-}, NO_3^-, and NH_4^+) are 0.06, 0.09, and 0.03 μg m^{-3}, respectively. MDL values ranged from 0.03 to 0.14 μg m^{-3} for trace aerosol species (Cl^-, Na^+, K^+, Mg^{2+}, and Ca^{2+}). MDL values for each species, and the percentage of PILS data above the MDL for each species and campaign are summarized in Table 1. MDL and precision (expressed as relative standard deviation, RSD) values for the samples collected in these campaigns using the URG system described below have been described in detail elsewhere (Yu et al., 2005; Yu et al., 2006).

To validate the blank-corrected semi-continuous PILS/IC chemical analysis results, time-integrated concentrations of key aerosol ion species were compared with blank-corrected 24 h integrated $PM_{2.5}$ samples collected by an annular denuder/filter-pack system (URG) for the major ionic species (SO_4^{2-}, NO_3^-, and NH_4^+). Briefly, the URG annular denuder/filter-pack system included a $PM_{2.5}$ cyclone (10 LPM), pre-filter denuders for capture of gaseous nitric acid, sulfur dioxide, and ammonia, and a Teflon filter for particle collection as well as a backup nylon filter and acid-coated denuder to capture any nitric acid or ammonia lost by volatilization from the particle collection filter, as described in detail elsewhere (Yu et al., 2005; Yu et al., 2006). Ion analysis of samples collected by the URG sampler was completed on two Dionex DX-500 ion chromatographs in our laboratory at Colorado State University. Particle concentrations of nitrate and ammonium were determined from the sum of material collected on the Teflon filter and the corresponding species measured on the backup filter or denuder (e.g., NH_4^+ from the Teflon filter plus NH_3 collected on the backup denuder).

We have previously reported on several aspects of aerosol composition for the numerous field campaigns described here. Engling et al. (2006) and Herckes et al. (2006) reported concentrations of organic biomass combustion markers measured in Yosemite to examine the influence of wildfires on regional haze. Yu et al. (2005, 2006) reported on nitrate quantification and ammonia loss for 24 h integrated aerosol samples collected on nylon filters. Lee et al. (2008) examined denuder/filter-pack, cascade impactor, and selected PILS measurements at these locations in order to assess the importance of fine vs. coarse particle nitrate at rural locations. Here our

Table 1
Summary of PILS Minimum Detection Limit (MDL) values for individual species and the percentage of data above MDL for each species and measurement campaign

Species	Overall MDL ($\mu g\,m^{-3}$)	Yosemite NP	San Gorgonio (April)	San Gorgonio (July)	Grand Canyon NP	Bondville	Brigantine National Wildlife Refuge	Great Smoky Mountains NP
		% > MDL						
Cl^-	0.082	60.2	53.9	34.1	34.3	61.4	68.4	28.1
NO_3^-	0.085	79.8	92.3	83.5	93.3	90.3	96.6	32.9
SO_4^{2-}	0.061	99.7	95.9	99.3	99.4	99.3	99.9	99.8
Na^+	0.027	89.9	77.0	82.1	81.0	99.7	22.5	19.8
NH_4^+	0.028	87.5	78.9	90.5	71.1	99.9	97.5	93.5
K^+	0.039	59.6	43.5	35.4	28.1	46.5	34.0	43.4
Mg^{2+}	0.027	52.2	66.3	52.2	22.3	26.6	30.6	23.8
Ca^{2+}	0.135	65.4	20.2	55.7	40.0	19.0	13.6	44.3

focus is on the sub-daily variability present in aerosol composition and concentration in rural environments and how such variability is tied to changes in transport and/or environmental conditions.

3. Results and discussion

The discussion begins with a validation of PILS results by comparison with 24 h integrated average major ion concentrations (NO_3^-, SO_4^{2-} and NH_4^+) measured using the denuder/filter-pack sampler. Next, we present PILS/IC semi-continuous aerosol composition measurements from the 6 study sites. As part of this discussion we examine the temporal variability in aerosol composition and concentration at each study location, look at how this variability is influenced by changes in transport patterns or environmental conditions, and consider relationships between individual ionic components that provide insight into the chemical forms of the major inorganic ion species.

3.1. Comparison of $PM_{2.5}$ filter-based and semi-continuous PILS measurements

$PM_{2.5}$ major ion (SO_4^{2-}, NO_3^-, and NH_4^+) concentrations measured using the PILS were averaged up to 24 h for comparison with 24 h integrated average concentrations of the same species measured using the URG denuder/filter-pack sampler. Only days where the PILS data covered more than 90% of the 24 h filter sampling period were included in the comparison. When observations from all study sites are included, the results from the two measurement techniques are in overall good agreement as shown in Fig. 2. The slopes (PILS vs. URG) of zero-intercept lines fit to the data set were 1.02, 0.95, and 0.97 for sulfate, nitrate, and ammonium with squared correlation coefficients (r^2) of 0.98, 0.96, and 0.92, respectively.

In comparing URG and PILS $PM_{2.5}$ SO_4^{2-}, NO_3^-, and NH_4^+ at individual sites (not shown), sulfate shows good agreement with linear regression slopes ranging from 0.94 to 1.08. Results for ammonium and nitrate are somewhat more scattered with individual site slopes (PILS vs. URG) ranging from 0.80 to 0.96 for ammonium and from 0.87 to 0.95 for nitrate with the PILS measurement biased low relative to the URG filter-pack measurement. The relatively poor agreement for ammonium may be due to difficulties in accurately measuring concentrations approaching the detection limit at many of these rural locations as well as ammonium volatilization in the PILS sampler (Orsini et al., 2003; Sorooshian et al., 2006). Because concentrations of other $PM_{2.5}$ ion species were generally low (typically$<0.2\ \mu g\,m^{-3}$), we don't present a full comparison of PILS vs. URG concentrations measured for these species. We (Malm et al., 2005) previously looked in detail at several different measurements of trace species in the field campaign with the largest data set at Yosemite National Park. We found strong correlation between PILS and URG K^+ ($r^2 = 0.90$), modest correlation for Na^+ ($r^2 = 0.64$), and low correlation for measurements of Cl^- and Ca^{2+} which were generally present at trace levels.

A summary of concentrations of $PM_{2.5}$ major ion components from the URG filter-pack and PILS sampler for individual sites is presented in Table 2. Not surprisingly, the variability in observed concentrations is much higher for the 15 min PILS data than for the 24 h URG filter-pack observations. For example, the relative standard deviations in nitrate concentrations measured by the PILS at San Gorgonio were 128% and 187% in April and July, respectively. The relative standard deviations of 24 h integrated average nitrate concentrations measured in the same periods were, by comparison, only 99% and 67%. As we turn to examine observations from individual measurement sites, we will see that large sub-daily variability in $PM_{2.5}$ species concentrations is often tied strongly to diurnally varying transport patterns.

3.2. Yosemite National Park, California (July–September 2002)

Average concentrations of $PM_{2.5}$ nitrate, sulfate, and ammonium measured with the PILS in Yosemite were 0.30, 1.0, and 0.36 $\mu g\,m^{-3}$ (see Table 1). Fig. 3 shows timelines of the concentrations of these three species along with non-sea salt (nss) K^+ (calculated using a sea water $[K^+]/[Na^+]$ ratio of 0.0128). Strong diurnal variability was observed in individual species concentrations, a pattern common at many elevated receptor sites. Daytime heating of the surface tends to destabilize the lower atmosphere and deepen the boundary layer, allowing pollutants emitted near the surface to mix to greater altitudes. In montane environments, direct solar heating of the mountain slope can warm air in contact with the surface. This warmer, more buoyant air tends to rise along the sloped

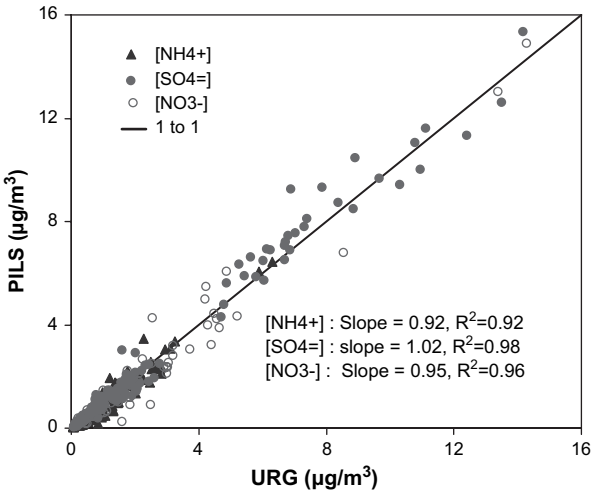

Fig. 2. Comparison of 24 h average concentrations of ammonium, sulfate, and nitrate measured by PILS/IC vs. concentrations measured with a URG denuder/filter-pack sampler.

surface producing a radiatively driven upslope flow. Both the deepening boundary layer and the upslope flow can bring pollutants from lower elevations to mountain monitoring sites. At night, surface cooling leads to downslope (drainage) flow as well as a shallower mixed layer. During the morning, concentrations of major ions often increased substantially at the Yosemite hillside measurement site within a half-hour of the onset of a thermally driven upslope flow. Lower concentrations usually prevailed during night-time drainage flows. Lower concentrations of sulfate were typically observed in August than in July. $PM_{2.5}$ K^+ concentrations were elevated during periods in mid- and late-August. Separate evidence indicates substantial air quality impacts from local and distant wildfires during study periods with elevated K^+ concentrations (Hand et al., 2005; McMeeking et al., 2005a, b, 2006; Engling et al., 2006).

The PILS data also provide interesting insight into $PM_{2.5}$ nitrate at Yosemite during the study. Nitrate concentrations are on average quite low, despite the location of Yosemite NP downwind of California's Central Valley, a region rich in NO_x emissions. Nitrate and ammonium appear to be closely coupled only during a few brief periods during the 2-month campaign. The low levels of particle phase ammonium nitrate reflect the thermodynamic equilibrium of the ammonia–nitric acid–ammonium nitrate system. When temperatures are high and relative humidities low, as experienced in Yosemite NP during summer, the equilibrium constant for ammonium nitrate formation decreases pushing the nitrogen speciation toward gas phase ammonia and nitric acid. Fig. 4 provides a closer view of PILS $PM_{2.5}$ nitrate, sodium, and chloride concentrations during a period from early August through early September. Note how concentrations of NO_3^- and Na^+ closely track one another. During periods when NO_3^- concentrations match or exceed Na^+ concentrations (e.g., much of the August 20–23 period), the aerosol is generally depleted of Cl^-. During periods when nitrate concentrations are lower than sodium concentrations (e.g., much of the August 7–13 period), some chloride remains in the particles. Note that the overall squared correlation coefficient (r^2) between Na^+ and Cl^- in this data is only 0.08.

Table 2
Statistical summary of $PM_{2.5}$ major ion concentrations ($\mu g\,m^{-3}$) measured using the URG and PILS samplers

Site		NO_3^- (p)				SO_4^{2-} (p)				NH_4^+ (p)			
		Mean	Min	Max	RSD*	Mean	Min	Max	RSD*	Mean	Min	Max	RSD*
Yosemite NP	URG	0.33	0.08	0.86	48	1.19	0.59	1.90	27	0.41	0.24	0.74	27
	PILS	0.30	0.01	3.25	71	1.01	0.20	2.66	42	0.36	0.001	1.30	45
San Gorgonio (April)	URG	3.35	0.17	14.56	99	0.80	0.22	1.48	131	1.33	0.17	4.71	79
	PILS	3.19	**	34.91	128	0.61	**	2.39	141	0.90	**	10.65	142
San Gorgonio (July)	URG	1.58	0.27	4.91	67	1.71	0.75	2.85	26	1.31	0.56	3.25	47
	PILS	1.29	**	20.22	187	1.33	**	6.90	52	0.95	**	7.22	104
Grand Canyon NP	URG	0.30	0.10	0.57	35	1.01	0.25	1.83	44	0.42	0.10	0.72	41
	PILS	0.26	**	1.46	91	1.03	0.01	2.98	109	0.41	**	1.41	98
Bondville	URG	4.87	1.63	14.48	66	2.88	0.55	6.89	71	2.35	0.67	6.40	63
	PILS	4.91	**	37.66	112	3.08	**	20.36	103	2.38	**	13.71	88
Brigantine	URG	1.26	0.49	3.70	62	2.27	0.63	4.70	53	1.32	0.42	3.19	51
	PILS	0.98	**	6.16	93	1.91	**	4.31	43	0.93	**	3.95	50
Great Smoky Mnts NP	URG	0.17	0.09	0.32	31	7.66	1.71	13.75	42	1.94	0.61	3.04	37
	PILS	0.16	**	2.25	130	7.74	**	19.74	51	1.69	**	3.89	54

*Relative Standard Deviation (RSD, %) = (Standard Deviation/Mean) × 100%; **Below Minimum Detection Limit (MDL).

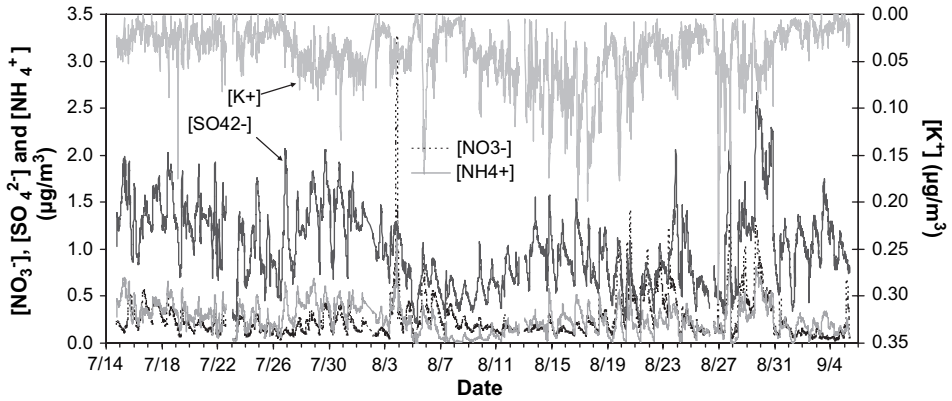

Fig. 3. 2002 Yosemite NP timelines of PILS $PM_{2.5}$ NO_3^-, SO_4^{2-}, NH_4^+, and K^+ concentrations. Note scale change (right axis) for K^+.

The squared correlation coefficient between Na^+ and NO_3^- is 0.45. When we compare Na^+ to the sum of NO_3^- and Cl^-, r^2 increases to 0.55. These patterns are evidence of displacement of chloride from sea salt particles, as a result of reaction with gas phase nitric acid or its precursors, during transport from the Pacific Ocean inland to Yosemite National Park.

3.3. San Gorgonio Wilderness Area, California (April & July 2003)

Aerosol concentrations at the San Gorgonio Wilderness Area have long been of particular interest due to its location along the northeastern edge of the Los Angeles air basin. Timelines of major ion concentrations (sulfate, nitrate, and ammonium) measured at San Gorgonio in April and July 2003 are shown in Fig. 5. Lower concentrations of the major ions were observed in mid-April and mid-July; periods of higher concentrations occurred in early April, and in early and late July. Sulfate was a relatively small contributor to $PM_{2.5}$ at San Gorgonio in April, with an average concentration measured by PILS of 0.61 $\mu g\,m^{-3}$. The average sulfate concentration measured in July increased to 1.33 $\mu g\,m^{-3}$. Formation of ammonium nitrate was favored during the relatively low temperatures and high humidities occurring in April, with an average PILS nitrate concentration of 3.19 $\mu g\,m^{-3}$. Unlike sulfate, the average nitrate concentration dropped in July to 1.29 $\mu g\,m^{-3}$. PILS nitrate concentrations exceeded 30 $\mu g\,m^{-3}$ during one period in April, and 20 $\mu g\,m^{-3}$ once in July at this wilderness area site. Other ion species (Na^+, K^+, Ca^{2+}, Mg^{2+} and Cl^-) were generally found to be minor contributors to total ion concentrations.

PILS measurements from San Gorgonio reveal diurnal concentration trends for many species, related to changes in atmospheric transport associated with daily mountain-valley wind circulations and changes in boundary layer depth. This pattern is especially apparent during the July measurement period as shown in Fig. 5B. Stronger, more regular diurnal trends were observed in July and large concentration peaks were registered daily during the afternoon after approximately 2:00 pm. The more regular pattern in July likely results from strengthening of the mountain-valley wind circulation and deeper boundary layer development associated with more intense summer solar radiation. The very high nitrate concentrations that were observed on April 9–10 were associated with passage of a strong low pressure trough. This trough, although it produced no significant precipitation, destabilized the boundary layer allowing regional emissions to mix to greater heights than normal.

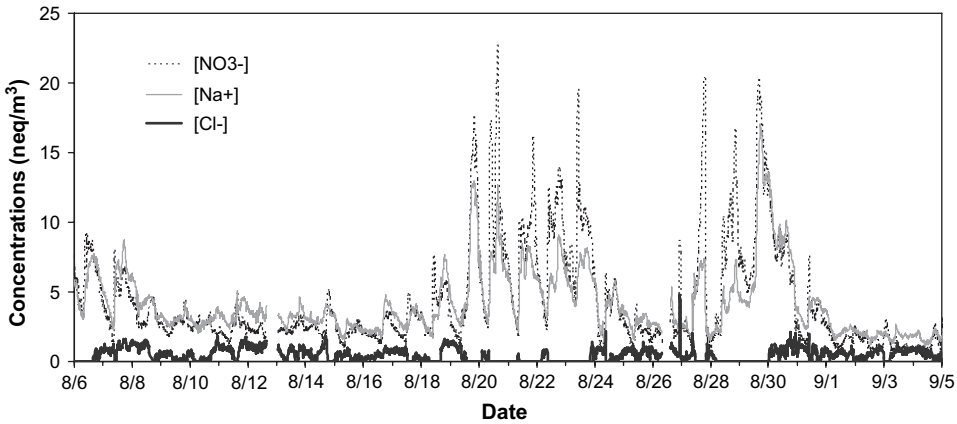

Fig. 4. Yosemite NP timelines of PILS $PM_{2.5}$ Cl^-, NO_3^-, and Na^+ concentrations from August 6 to September 4, 2002.

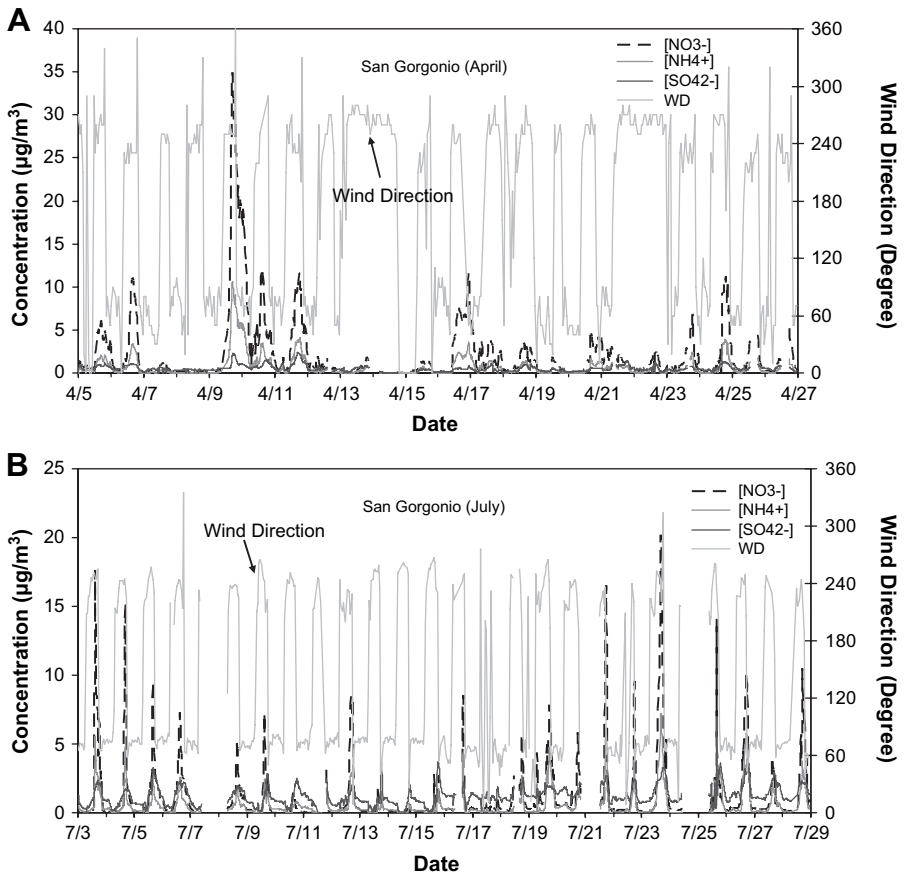

Fig. 5. 2003 San Gorgonio Wilderness Area timelines of PILS $PM_{2.5}$ NO_3^-, SO_4^{2-}, and NH_4^+ concentrations and wind direction.

A closer look at the San Gorgonio PILS timeline in July provides interesting insight into factors controlling the timing of individual ion concentration peaks. An example is shown in Fig. 6, where peaks in nitrate and sulfate concentrations were observed during the afternoon with upslope transport of air to the site. Following the return to downslope flow around 6:00 pm, a lag is seen before the sulfate concentration drops off. We interpret this lag as the time required for the downslope flow to carry the polluted air mass back past the site to lower elevations. The nitrate concentration, by contrast, decreases even before the wind reverses from upslope to downslope. This is consistent with loss of particulate ammonium nitrate to the gas phase as afternoon temperatures warm (see Fig. 6). Some of the particulate nitrate loss probably occurs at lower altitude, where temperatures are even warmer. A high dry deposition velocity of gaseous nitric acid likely leads to rapid depletion of nitric acid from the air mass in contact with the forested mountain slopes once the ammonium nitrate volatilizes. Some evidence of nitric acid reaction with sea salt is also present in the San Gorgonio PILS data. During July, in particular, Na^+ concentrations measured at the site substantially exceed Cl^- concentrations. As at Yosemite, this suggests the importance of sea salt chloride loss by acid displacement reactions of sea salt with nitric acid or its precursors.

Fig. 7 depicts the timeline of nss-K^+ concentrations over the course of July at San Gorgonio. Periods of elevated K^+ suggest that fires significantly impacted the sampling site on July 5–6, 17–19, and 26. The PILS K^+ spikes are consistent with high concentrations of K^+, also observed in URG filter samples on July 5, 17, 18, and 19 (not shown). The K^+ concentration spike observed on July 26 at San Gorgonio demonstrates, for example, how highly time-resolved measurements can provide insight into even brief plumes of aerosol advected to the site. July is wildfire season in southern California and fires were burning in the region during the study. No smoke impacts were evident during the April study.

3.4. Grand Canyon National Park, Arizona (May 2003)

Fig. 8 depicts timelines of PILS $PM_{2.5}$ SO_4^{2-}, NO_3^-, and NH_4^+ measured in Grand Canyon National Park. Low concentrations were observed in early May, increasing by mid-month. PILS concentrations of $PM_{2.5}$ nitrate, sulfate, and ammonium averaged 0.26, 1.03, and 0.41 $\mu g\,m^{-3}$ during the study period. Most ammonium in fine particles at this location appears to be associated with sulfate, with a sulfate to ammonium ratio close to 1 on a charge equivalent concentration basis as shown in Fig. 8. While nitrate concentrations were low during the study, note that the

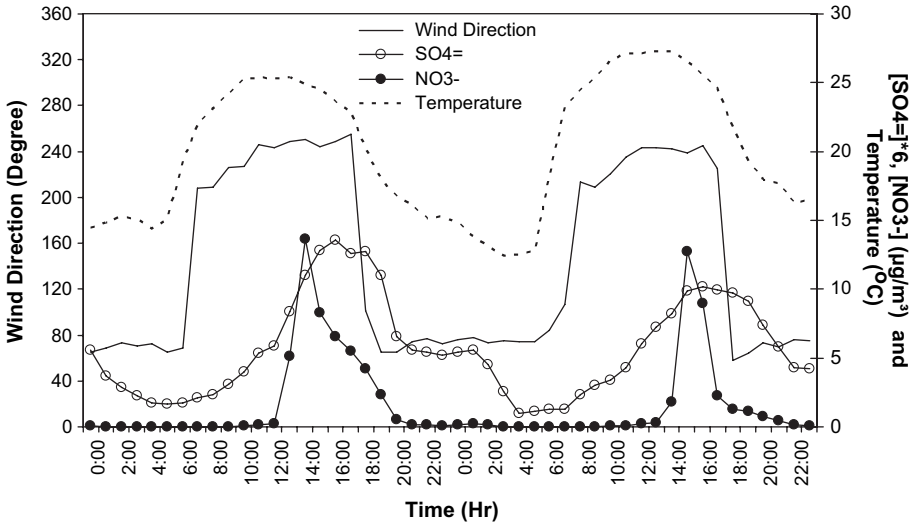

Fig. 6. Example PILS NO_3^-, and SO_4^{2-} timelines with wind direction and temperature at San Gorgonio (July).

sum of nitrate and sulfate concentrations exceeds the ammonium concentration. Once again this suggests that the nitrate may be present in forms other than ammonium nitrate. Nitric acid reaction with soil particles is a possibility (Cheng et al., 2000; Evans et al., 2004; Finlayson-Pitts and Pitts, 2000; Goodman et al., 2000; Grassian, 2002; Hanisch and Crowley, 2001a; Hanisch and Crowley, 2001b; Hanisch and Crowley, 2003; Ooki and Uematsu, 2005; Pakkanen, 1996; Underwood et al., 2001). Fig. 9 compares timelines of $PM_{2.5}$ NO_3^- with Na^+ and Ca^{2+}, which typically are associated with sea salt and soil dust. Close tracking of NO_3^- with some of these other species is supportive of a hypothesis of nitric acid reaction with coarse mode, alkaline particles. This issue is explored in more detail elsewhere (Lee et al., 2008), where species' particle size distributions are also compared.

3.5. Bondville, Illinois (February 2003)

Sulfate, nitrate, and ammonium were the dominant ionic species during winter measurements at the mid-western Bondville site. Concentrations of sulfate, nitrate, and ammonium ranged from 0.02 to 30.4 $\mu g\,m^{-3}$, 0.01 to 37.7 $\mu g\,m^{-3}$, and 0.01 to 13.7 $\mu g\,m^{-3}$, respectively, with the highest concentrations occurring at the end of study (see Fig. 10). The high time resolution nitrate and sulfate measurements at Bondville give interesting insights into ambient aerosol behavior. Observations from noon February 17 to midnight on the following day, and again during the afternoon of February 21, revealed rapid transitions between nitrate and sulfate dominated aerosols. Fig. 11 highlights a transient sulfate episode in the February 17–19 period. Changes during this time period are consistent with thermodynamic expectations for the ammonia–nitric acid–sulfuric acid system, which indicate that ammonium nitrate should form in an internally mixed aerosol only when sufficient ammonia is present to first fully neutralize sulfate (Seinfeld and Pandis, 2006). A sulfate-rich air mass passed over the sampling site when the wind shifted from northeasterly to more southwesterly. As sulfate concentrations rose, they reached a point where insufficient ammonia was available to neutralize the

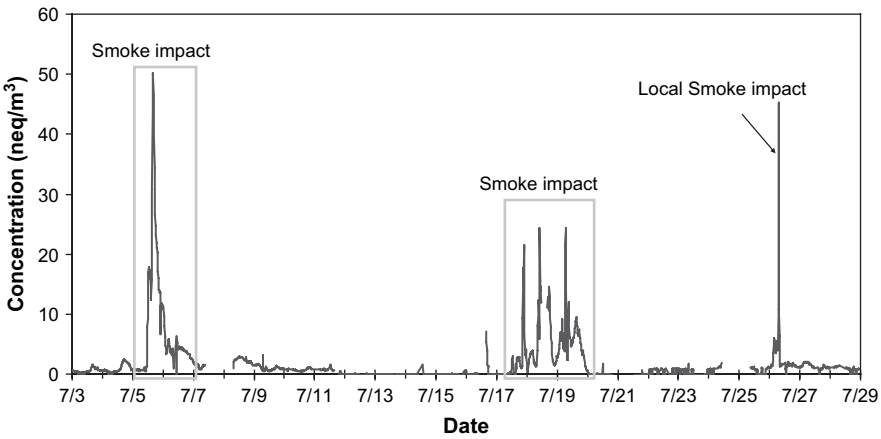

Fig. 7. Timeline of $PM_{2.5}$ nss-K^+ ion concentrations measured in July 2003 at San Gorgonio.

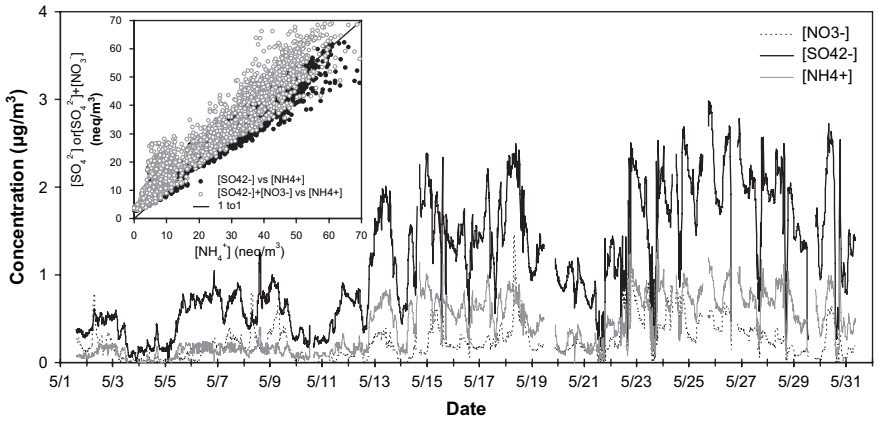

Fig. 8. 2003 Grand Canyon NP timelines of PILS $PM_{2.5}$ concentrations of sulfate, nitrate, and ammonium. Ratios of $PM_{2.5}$ sulfate or sulfate + nitrate to ammonium are shown in the inset.

aerosol and nitrate concentrations decreased. The nitrate concentration decrease is consistent with nitrate being forced back to its gas phase form, nitric acid. Later on February 18, the $[NH_4^+]/[SO_4^{2-}]$ ratio (not shown) rose as sulfate concentrations decreased. Once the aerosol was neutralized, NH_4NO_3 was observed to form again.

The high measurement time resolution makes PILS data especially useful for looking at how concentrations change with meteorological conditions. As an example of this we examined variability in nitrate and sulfate concentrations, with wind direction, for the Bondville measurement campaign. A Conditional Probability Function (CPF) was used to identify transport patterns associated with high concentrations of nitrate and sulfate. Our analysis follows approaches previously outlined elsewhere (Kim et al., 2003; Xie and Berkowitz, 2006). The CPF is defined as $CPF = m_\theta/n_\theta$, where m_θ is the number of samples in a 10° wind sector θ with concentrations of sulfate (or nitrate) greater than the 75th percentile of all study sulfate (or nitrate) observations, and n_θ is the total number of samples in the same wind sector θ. CPF plots are included in Fig. 12 for nitrate and sulfate. These can be interpreted as showing the likelihood that air arriving from a particular direction contains some of the highest nitrate or sulfate concentrations observed during the campaign. The patterns for nitrate and sulfate overlap some but are overall rather different. High nitrate concentrations were fairly common when the wind at Bondville blew from the east or northeast. This might reflect, in part, the location of the Bondville site several kilometers west of the cities of Champaign and Urbana, Illinois, but also might reflect the general increase in regional NO_x emissions as one moves east of the sampling region. High sulfate concentrations, by contrast, were most common when the wind blew from the east/southeast or from the south/southwest. Both directions reflect upwind regions where sulfur dioxide emissions are large. Because measured sulfate and nitrate are both secondary species, and because local winds don't always represent regional transport well, we should be cautious not to over-interpret the plots in Fig. 12. This is especially true for nitrate, due to its semi-volatile nature and tendency to move between the gas and particle phases depending on the relative availability of ammonia and sulfate and on temperature and relative humidity. Nevertheless, these CPF plots do provide some interesting insight into conditions which produced high concentrations of

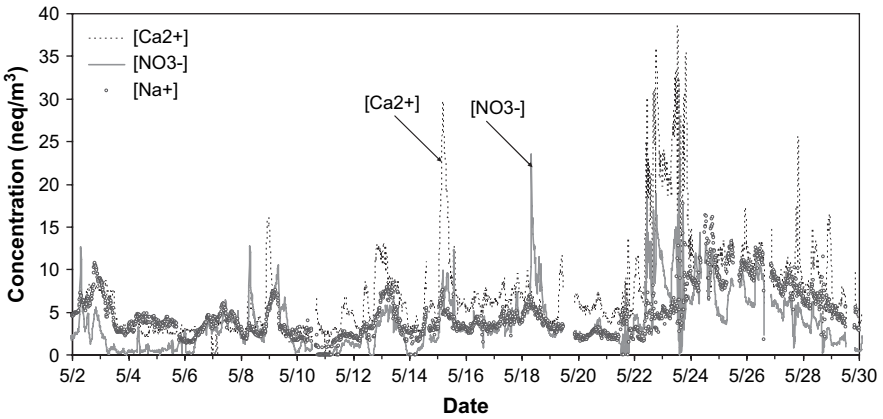

Fig. 9. 2003 Grand Canyon NP timelines of $PM_{2.5}$ PILS NO_3^-, Ca^{2+}, and Na^+ concentrations.

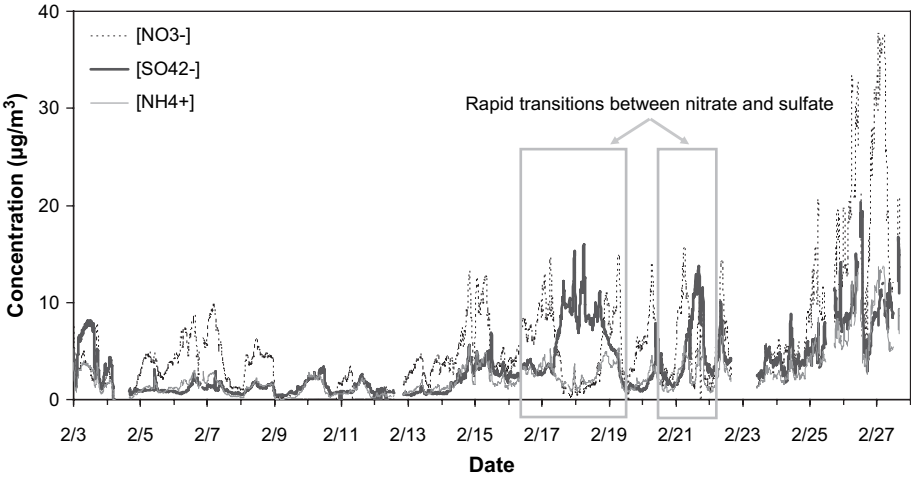

Fig. 10. 2003 Bondville, Illinois timelines of PILS $PM_{2.5}$ NO_3^-, SO_4^{2-}, and NH_4^+ concentrations.

sulfate and nitrate during the Bondville campaign and help illustrate the utility of high time resolution $PM_{2.5}$ composition measurements.

3.6. Brigantine National Wildlife Refuge, New Jersey (November 2003)

Fig. 13 shows timelines of the major ion species measured by PILS at the Brigantine National Wildlife Refuge, New Jersey in November 2003. Concentrations are plotted in Fig. 13 in units of nanoequivalents m^{-3} (neq m^{-3}), in order to illustrate the relative charge balance between NO_3^-, SO_4^{2-}, and NH_4^+. Mass concentrations of NO_3^-, SO_4^{2-}, and NH_4^+ ranged from below detection limit to 4.3, 6.2, and 3.0 µg m^{-3}, respectively. As at Bondville, fine particles at Brigantine were sometimes nitrate-dominated and at other times dominated by sulfate. Nitrate concentration spikes were generally of shorter duration than periods of elevated sulfate. This is reflected by the greater concentration variability measured with the PILS for nitrate (rsd = 93%) than for sulfate (rsd = 43%).

Comparison of $PM_{2.5}$ ammonium, nitrate, and sulfate concentrations indicates that during most time periods ammonium was roughly balanced by the sum of nitrate and sulfate concentrations. Some periods were observed, however, where insufficient ammonium was found in the aerosol to neutralize even the sulfate present. For example, during much of the day on November 19, sulfate concentrations were much higher than ammonium concentrations, while nitrate concentrations were very low. On November 26, by contrast, ammonium was in balance with comparable amounts of nitrate and sulfate. Several periods are observed (e.g., on November 7 and on November 29) where very similar levels of ammonium and sulfate are observed, but nitrate concentrations are low.

K^+, Mg^{2+}, and Ca^{2+} were found to be present at very low concentrations (close to the detection limits) on most days. By contrast, $PM_{2.5}$ Na^+ and Cl^- concentrations (see Fig. 14) were relatively high during much of the study, even in the $PM_{2.5}$ fraction, reflecting this measurement site's proximity to the Atlantic Ocean. A scattering of Cl^-/Na^+ ratios around the expected value of 1.164 for sea water (see Fig. 14 inset)

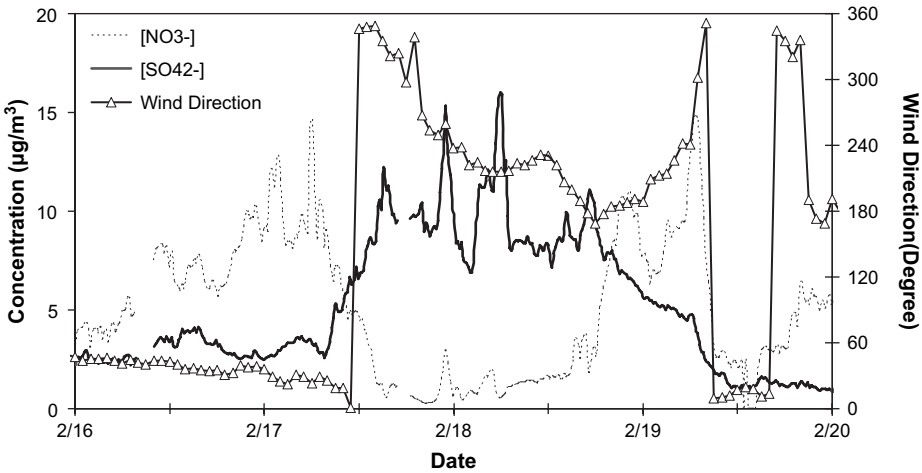

Fig. 11. Timelines of PILS $PM_{2.5}$ NO_3^- and SO_4^{2-} concentrations and wind direction at the Bondville site from February 16 to February 20, 2003.

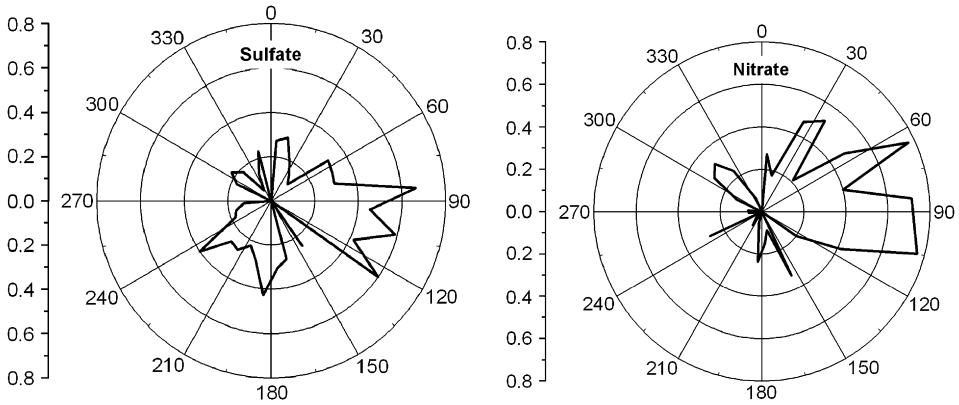

Fig. 12. CPF plots of the sulfate and nitrate at the Bondville site.

indicates the relatively unaged nature of sea salt aerosol found at this coastal site. A few episodes where chloride is observed without a sodium counter-ion correspond to periods when calculated back-trajectories indicate transport to the site was from inland locations, suggesting possible contributions by other chloride sources in the region.

3.7. Great Smoky Mountains National Park, Tennessee (July/August 2004)

Fig. 15 shows timelines of PILS $PM_{2.5}$ sulfate, nitrate, and ammonium concentrations measured in Great Smoky Mountains National Park in summer 2004. As expected (Olszyna et al., 2005), summertime aerosol at this site was observed to be strongly sulfate dominated with concentrations during several periods reaching 15 $\mu g\,m^{-3}$ or more. Ammonium concentrations ranged from below detection limit to 3.8 $\mu g\,m^{-3}$. The average ammonium concentration was 1.69 $\mu g\,m^{-3}$ vs. 7.74 $\mu g\,m^{-3}$ for sulfate. Generally, ammonium concentration trends were moderately correlated to sulfate trends. Ratios of SO_4^{2-} to NH_4^+ concentrations indicated an aerosol that was nearly always acidic (Fig. 15 inset). Molar ratios of $[NH_4^+]/[SO_4^{2-}]$ are presented as a timeline in Fig. 16. The ratio shows considerable variability during the study, but only rarely reached 2.0, the aerosol neutral point. Molar ratios ranged from 0.05 to 3.56 with an average of 1.19. Generally one sees a trend toward lower $[NH_4^+]/[SO_4^{2-}]$ molar ratios at higher sulfate concentrations, suggesting that aerosol acidity at the site typically increases with the amount of sulfate. One consequence of the acidic nature of the aerosol is that the formation of particulate ammonium nitrate is not favored thermodynamically (Karlsson and Ljungstrom, 1998; Lee et al., 2004; Seinfeld and Pandis, 2006). Observed nitrate concentrations were almost always well below 1 $\mu g\,m^{-3}$, averaging only 0.16 $\mu g\,m^{-3}$.

The relationship between sulfate concentration and local transport at the site was examined (not shown) (Lee, 2007). Sulfate temporal trends are correlated with the wind pattern at the site. Boundary layer breakup (or growth) starts in the early morning with more polluted air typically reaching the site in the early afternoon. Increases in sulfate concentration are typically observed between the hours of 2 and 4 pm. Generally, winds shifted from northerly or northwesterly (upslope) to southerly or

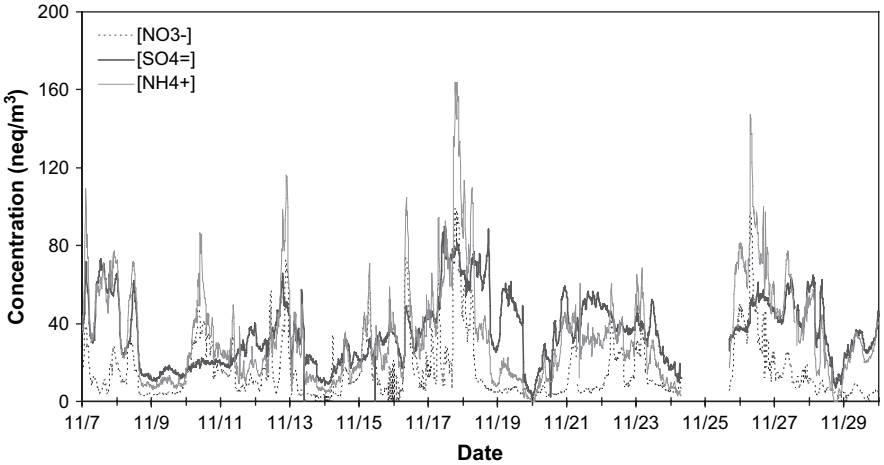

Fig. 13. 2003 Brigantine NWR timelines of PILS $PM_{2.5}$ NO_3^-, SO_4^{2-}, and NH_4^+ concentrations.

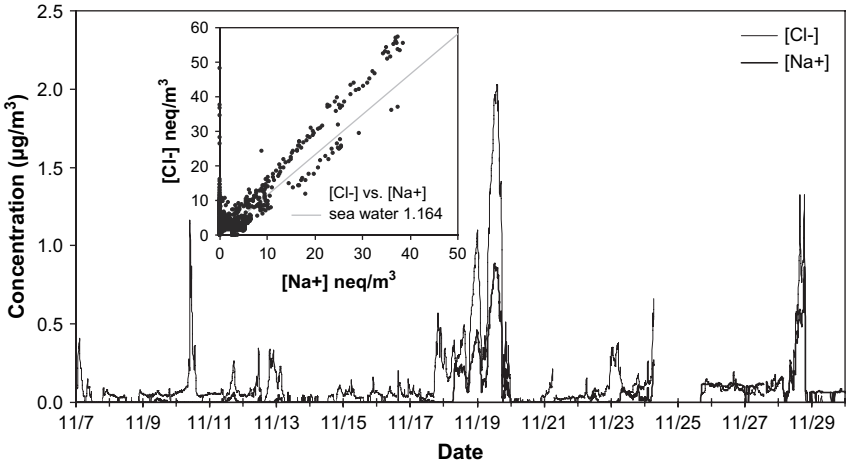

Fig. 14. 2003 Brigantine NWR timelines of PILS $PM_{2.5}$ Cl^- and Na^+ concentrations. The inset shows the relationship between Cl^- and Na^+.

southeasterly (downslope) around sunset, accompanied by a decrease in sulfate concentrations. As at other mountain sites (Yosemite, San Gorgonio), changes in transport driven by thermally induced mountain-valley wind circulations play an important role in diurnally varying pollutant concentrations at the site.

4. Summary and conclusions

The chemical composition of $PM_{2.5}$ and its temporal variability at 15 min time resolution were measured by PILS/IC at six rural locations in the United States during different seasons (Bondville, IL, in winter; San Gorgonio Wilderness Area, CA, and Grand Canyon NP, AZ, in spring; Yosemite NP, San Gorgonio Wilderness Area, CA, and Great Smoky Mountains NP, TN, in summer; Brigantine, NJ, in fall). The variability in both aerosol composition and aerosol concentration provide considerable insight into processes controlling aerosol characteristics at these rural locations.

Strong diurnal concentration trends of many $PM_{2.5}$ ion species were clearly correlated with changing transport patterns at several locations. Thermally driven mountain-valley wind systems, for example, were observed to influence aerosol concentrations at several sites in complex terrain, including Yosemite National Park, San Gorgonio Wilderness Area, and Great Smoky Mountains National Park. Peak concentrations at these sites were generally observed during daytime, upslope transport, with lower concentrations prevailing during night-time drainage flow. 24 h average samples, of course, do not capture patterns of this type and, consequently, fail to capture peak fine particle concentrations observed in these locations. At the San Gorgonio site, for example, the peak 15 min $PM_{2.5}$ nitrate concentration was 34.9 $\mu g\,m^{-3}$, 2.4 times the highest daily average concentration at the site. In the July San Gorgonio measurement period, the peak 15 min nitrate concentration was more than four times the highest daily average. Ratios between nitrate 15 min and 24 h maximum concentrations

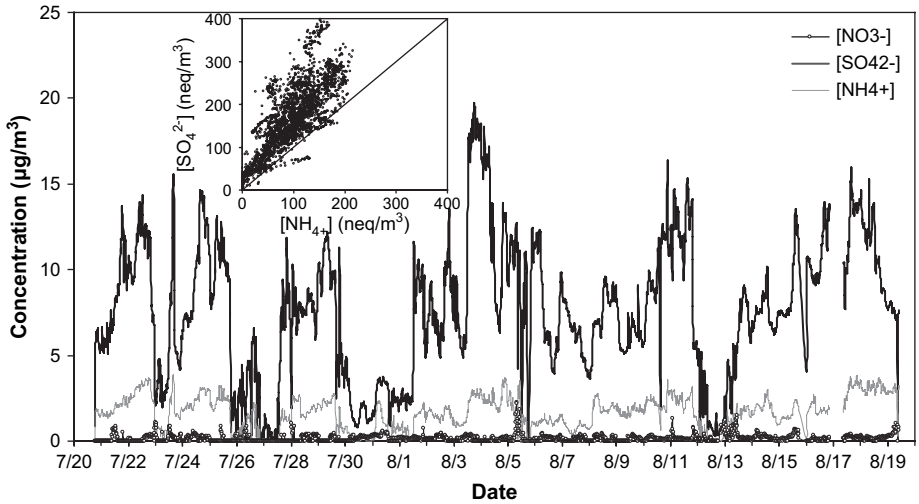

Fig. 15. 2004 Great Smoky Mountains NP timelines of PILS $PM_{2.5}$ NO_3^-, SO_4^{2-}, and NH_4^+ concentrations. The inset shows the relationship between SO_4^{2-} and NH_4^+ concentrations.

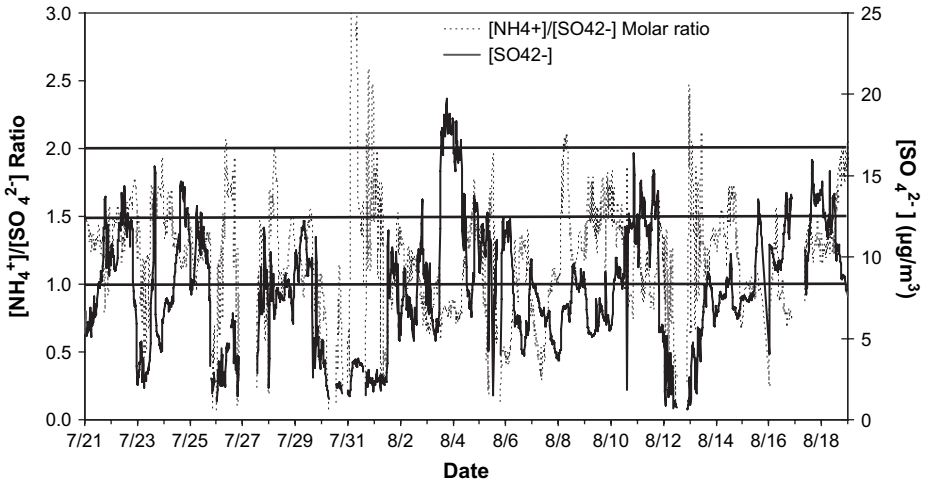

Fig. 16. 2004 Great Smoky Mountains NP timelines of the PILS $PM_{2.5}$ NH_4^+/SO_4^{2-} molar ratio and the sulfate concentration.

at Yosemite and Great Smoky Mountains National Parks were also large at 3.8 and 7.0, respectively. Differences between 15 min and 24 h maximum concentrations were not as large for sulfate, perhaps reflecting a more regional nature of this pollutant species.

High time resolution aerosol composition measurements also provide increased insight into relationships between individual aerosol ion components and the influence of environmental conditions on aerosol chemistry. Observations from Bondville, Illinois, revealed rapid transitions between nitrate and sulfate dominated aerosols, and suggested that particle nitrate formation strongly depends on aerosol acidity. The gas-particle partitioning of ammonium nitrate was also clearly seen in San Gorgonio where concentrations of $PM_{2.5}$ nitrate rapidly disappeared as temperatures rose during warm summer afternoons. Formation of nitrate by reactions of nitric acid or its precursors with soil dust and sea salt were also evident based on correlations between nitrate concentrations and concentrations of key sea salt and soil dust species, including Na^+, Cl^- and Ca^{2+}. Observations at Yosemite, for example, clearly showed that $PM_{2.5}$ nitrate during summer was usually present as a result of nitrate displacement of chloride from sea salt.

Observations of $PM_{2.5}$ K^+ also provided insight into periods when sampling sites were impacted by smoke from local and/or distant biomass fires. Fire impact periods were observed in summertime at both the Yosemite and San Gorgonio sites. One advantage of high time resolution PILS K^+ measurements is the ability to detect even brief smoke plume impacts at the site that would be impossible to discern from 24 h integrated measurements.

High time resolution measurements of multiple aerosol chemical constituents are at present practical in most cases only in short duration research studies. Given the value of such observations in improving our understanding of peak aerosol concentrations and of factors influencing both aerosol concentrations and composition, however, we believe priority needs to be placed on developing approaches to permit high time resolution measurements on a more routine basis.

Acknowledgements

The authors thank the National Park Service for financial support of this work. We thank C. McDade and the IMPROVE team at UC Davis for outstanding support in field support preparation and study logistics. We also thank B. Ayres, J. Carrillo, and C. Hale of CSU for assistance with field campaign planning and preparations. We are grateful to numerous individuals working at each of the field sites for providing site access and/or logistical assistance, including M. Snider in Bondville, H. Abreu at Grand Canyon, M. Arbough and D. Jones at San Gorgonio, S. Perchetti at Brigantine, and J. Renfro and B. Stroik at Great Smoky Mountains.

References

Adams, P.J., Seinfeld, J.H., Koch, D.M., 1999. Global concentrations of tropospheric sulfate, nitrate, and ammonium aerosol simulated in a general circulation model. Journal of Geophysical Research 104 (D11), 13791–13823.

Allegrini, I., Febo, A., Perrino, C., Masia, P., 1994. Measurement of atmospheric nitric-acid in gas-phase and nitrate in particulate matter by means of annular denuders. International Journal of Environmental Analytical Chemistry 54 (3), 183–201.

Appel, B.R., 1993. Sampling of selected labile atmospheric pollutants. Advances in Chemistry Series (232), 1–40.

Appel, B.R., Tokiwa, Y., 1981. Atmospheric particulate nitrate sampling errors due to reactions with particulate and gaseous strong acids. Atmospheric Environment 15 (6), 1087–1089.

Buhr, S.M., Buhr, M.P., Fehsenfeld, F.C., Holloway, J.S., Karst, U., Norton, R.B., Parrish, D.D., Sievers, R.E., 1995. Development of a semicontinuous method for the measurement of nitric-acid vapor and particulate nitrate and sulfate. Atmospheric Environment 29 (19), 2609–2624.

Cheng, M.D., Tanner, R.L., 2002. Characterization of ultrafine and fine particles at a site near the Great Smoky Mountains National Park. Atmospheric Environment 36 (38), 5795–5806.

Cheng, Z.L., Lam, K.S., Chan, L.Y., Wang, T., Cheng, K.K., 2000. Chemical characteristics of aerosols at coastal station in Hong Kong. I. Seasonal variation of major ions, halogens and mineral dusts between 1995 and 1996. Atmospheric Environment 34, 2771–2783.

Chow, J.C., Watson, J.G., Lowenthal, D.H., Magliano, K.L., 2005. Loss of $PM_{2.5}$ nitrate from filter samples in central California. Journal of The Air & Waste Management Association 55 (8), 1158–1168.

Dentener, F.J., Carmichael, G.R., Qhang, Y., Lelieveld, J., Crutzen, P.J., 1996. Role of mineral aerosol as a reactive surface in the global troposphere. Journal of Geophysical Research 101 (D17), 22869–22889.

Engling, G., Herckes, P., Kreidenweis, S., Malm, W.C., Collett Jr., J.L., 2006. Composition of the fine organic aerosol in Yosemite National Park during the 2002 Yosemite Aerosol Characterization Study. Atmospheric Environment 40, 2959–2972.

Evans, M.S.C., Campbell, S.W., Bhethanabotla, V., Poor, N.D., 2004. Effect of sea salt and calcium carbonate interactions with nitric acid on the direct dry deposition of nitrogen to Tampa Bay, Florida. Atmospheric Environment 38 (29), 4847–4858.

Finlayson-Pitts, B.J., Pitts, J.N.J., 2000. Chemistry of the Upper and Lower Atmosphere. Academic Press.

Goodman, A.L., Underwood, G.M., Grassian, V.H., 2000. A laboratory study of the heterogenous reaction of nitric acid on calcium carbonate particles. Journal of Geophysical Research 105 (D23), 29053–29064.

Grassian, V.H., 2002. Chemical reactions of nitrogen oxides on the surface of oxide, carbonate, soot, and mineral dust particles: implications for the chemical balance of the troposphere. Journal of Physical Chemistry A 106 (6), 860–877.

Hand, J.L., Malm, W.C., Laskin, A., Day, D., Lee, T., Wang, C., Carrico, C., Carrillo, J., Cowin, J.P., Collett Jr., J.L., Iedema, M.J., 2005. Optical, physical, and chemical properties of tar balls observed during the Yosemite Aerosol Characterization Study. Journal of Geophysical Research-Atmospheres 110 (D21), D21210, doi:10.1029/2004JD005728.

Hanisch, F., Crowley, J.N., 2001a. Heterogeneous reactivity of gaseous nitric acid on Al_2O_3, $CaCO_3$, and atmospheric dust samples: a Knudsen cell study. Journal of Physical Chemistry A 105 (13), 3096–3106.

Hanisch, F., Crowley, J.N., 2001b. The heterogeneous reactivity of gaseous nitric acid on authentic mineral dust samples, and on individual mineral and clay mineral components. Physical Chemistry Chemical Physics 3 (12), 2474–2482.

Hanisch, F., Crowley, J.N., 2003. Heterogeneous reactivity of NO and HNO_3 on mineral dust in the presence of ozone. Physical Chemistry Chemical Physics 5 (5), 883–887.

Herckes, P., Engling, G., Kreidenweis, S.M., Collett Jr., J.L., 2006. Particle size distributions of organic aerosol constitutents during the 2002 Yosemite Aerosol Characterization Study. Environmental Science & Technology 40, 4554–4562.

Hering, S., Cass, G., 1999. The magnitude of bias in the measurement of $PM_{2.5}$ arising from volatilization of particulate nitrate from teflon filters. Journal of the Air & Waste Management Association 49 (6), 725–733.

Hering, S.V., Lawson, D.R., Allegrini, I., Febo, A., Perrino, C., Possanzini, M., Sickles, J.E., Anlauf, K.G., Wiebe, A., Appel, B.R., John, W., Ondo, J., Wall, S., Braman, R.S., Sutton, R., Cass, G.R., Solomon, P.A., Eatough, D.J., Eatough, N.L., Ellis, E.C., Grosjean, D., Hicks, B.B., Womack, J.D., Horrocks, J., Knapp, K.T., Ellestad, T.G., Paur, R.J., Mitchell, W.J., Pleasant, M., Peake, E., Maclean, A., Pierson, W.R., Brachaczek, W., Schiff, H.I., Mackay, G.I., Spicer, C.W., Stedman, D.H., Winer, A.M., Biermann, H.W., Tuazon, E.C., 1988. The nitric-acid shootout–field comparison of measurement methods. Atmospheric Environment 22 (8), 1519–1539.

Jacobson, M.Z., 2001. Global direct radiative forcing due to multicomponent anthropogenic and natural aerosols. Journal of Geophysical Research 106 (D2), 1551–1568.

John, W., Wall, S.M., Ondo, J.L., Winklmayr, W., 1990. Modes in the size distributions of atmospheric inorganic aerosol. Atmospheric Environment 24A (9), 2349–2359.

Karlsson, A., Irgum, K., Hansson, H.C., 1997. Single-stage flowing liquid film impactor for continuous on-line particle analysis. Journal of Aerosol Science 28 (8), 1539–1551.

Karlsson, R., Ljungstrom, E., 1998. A laboratory study of the interaction of NH_3 and NO_2 with sea salt particles. Water, Air and Soil Pollution 103 (1–4), 55–70.

Kim, E., Hopke, P.K., Edgerton, E., 2003. Source identification of Atlanta aerosol by positive matrix factorization. Journal of the Air & Waste Management Association 53, 731–739.

Khlystov, A., Wyers, G.P., Slanina, J., 1995. The steam-jet aerosol collector. Atmospheric Environment 29 (17), 2229–2234.

Koutrakis, P., Thompson, K.M., Wolfson, J.M., Spengler, J.D., Keeler, G.J., Slater, J.L., 1992. Determination of aerosol strong acidity losses due to interactions of collected particles: results from laboratory and field studies. Atmospheric Environment 26A (6), 987–995.

Laskin, A., Wietsma, T.W., Krueger, B.J., Grassian, V.H., 2005. Heterogeneous chemistry of individual mineral dust particles with nitric acid: a combined CCSEM/EDX, ESEM, and ICP-MS study. Journal of Geophysical Research 110 (D10), D10208, doi:10.1029/2004JD005206.

Lee, H.S., Wadden, R.A., Scheff, P.A., 1993. Measurement and evaluation of acid air pollutants in Chicago using an annular denuder system. Atmospheric Environment 27A, 543–553.

Lee, T., 2007. Characterizing ionic components of aerosol in rural environments: temporal variability, size distributions, and the form of particle nitrate. PhD. thesis, Colorado State University, Fort Collins.

Lee, T., Kreidenweis, S.M., Collett Jr., J.L., 2004. Aerosol ion characteristics during the Big Bend Regional Aerosol and Visibility Observational Study. Journal of Air & Waste Management Association 54, 585–592.

Lee, T., Yu, X.-Y., Ayres, B., Kreidenweis, S.M., Malm, W.C., Collett Jr., J.L., 2008. Observation of fine and coarse particle nitrate at several rural locations in the United States. Atmospheric Environment 42 (11), 2720–2732.

Malm, W.C., Schichtel, B.A., Pitchford, M.L., Ashbaugh, L.L., Eldred, R.A., 2004. Spatial and monthly trends in speciated fine particle concentration in the United States. Journal of Geophysical Research-Atmospheres 109, D03306, doi:10.1029/2003JD003739.

Malm, W.C., Day, D.E., Carrico, C., Kreidenweis, S.M., Collett Jr., J.L., McMeeking, G., Lee, T., Carrillo, J., 2005. Intercomparison and closure calculations using measurements of aerosol species and optical properties during the Yosemite Aerosol Characterization Study. Journal of Geophysical Research 110, D14302, doi:10.1029/2004JD005494.

Malm, W.C., Sisler, J.F., Huffman, D., Eldred, R.A., Cahill, D.M., 1994. Spatial and seasonal trends in particle concentration and optical extinction in the United States. Journal of Geophysical Research 99 (D1), 1347–1370.

McMeeking, G.R., Kreidenweis, S.M., Carrico, C.M., Collett Jr., J.L., Day, D.E., Malm, W.C., 2005a. Observations of smoke-influenced aerosol during the Yosemite Aerosol Characterization Study: 2. Aerosol scattering and absorbing properties. Journal of Geophysical Research-Atmospheres 110 (D18), D18209, doi:10.1029/2004JD005389.

McMeeking, G.R., Kreidenweis, S.M., Carrico, C.M., Lee, T., Collett Jr., J.L., Malm, W.C., 2005b. Observations of smoke-influenced aerosol during the Yosemite Aerosol Characterization Study: size distributions and chemical composition. Journal of Geophysical Research-Atmospheres 110 (D9), D09206, doi:10.1029/2004JD005389.

McMeeking, G.R., Kreidenweis, S.M., Lunden, M., Carrillo, J., Carrico, C.M., Lee, T., Herckes, P., Engling, G., Day, D.E., Hand, J., Brown, N., Malm, W. C., Collett Jr., J.L., 2006. Smoke-impacted regional haze in California during the summer of 2002. Agricultural and Forest Meteorology 137 (1–2), 25–42.

Nel, A., 2005. Air pollution-related illness: effects of particles. Science 308, 804–806.

Olszyna, K.J., Bairai, S.T., Tanner, R.L., 2005. Effect of ambient NH_3 levels on $PM_{2.5}$ composition in the Great Smoky Mountains National Park. Atmospheric Environment 39 (25), 4593–4606.

Oms, M.T., Jongejan, P.A.C., Veltkamp, A.C., Wyers, G.P., Slanina, J., 1996. Continuous monitoring of atmospheric HCl, HNO_2, HNO_3, and SO_2, by wet-annular denuder air sampling with on-line chromatographic analysis. International Journal of Environmental Analytical Chemistry 62 (3), 207–218.

Ooki, A., Uematsu, M., 2005. Chemical interactions between mineral dust particles and acid gases during Asian dust events. Journal Of Geophysical Research-Atmospheres 110 (D3), D03201, doi:10.1029/2004JD004737.

Orsini, D.A., Ma, Y.L., Sullivan, A., Sierau, B., Baumann, K., Weber, R.J., 2003. Refinements to the particle-into-liquid sampler (PILS) for ground and airborne measurements of water soluble aerosol composition. Atmospheric Environment 37 (9–10), 1243–1259.

Padgett, P.E., Bytnerowicz, A., 2001. Depostion and adsorption of the air pollutant HNO_3 vapor to soil surfaces. Atmospheric Environment 35 (13), 2405–2415.

Pakkanen, T.A., 1996. Study of formation of coarse particle nitrate aerosol. Atmospheric Environment 30 (14), 2475–2482.

Pakkanen, T.A., Kerminen, V.-M., Hillamo, R.E., Makinen, M., Makela, T., Virkkula, A., 1996. Distribution of nitrate over sea-salt and soil derived particles-implications from a field study. Journal of Atmospheric Chemistry 24, 189–205.

Pang, Y., Ren, Y., Obeidi, F., Hastings, R., Eatough, D.J., Wilson, W.E., 2001. Semi-volatile species in $PM_{2.5}$: comparison of integrated and continuous samplers for $PM_{2.5}$ research or monitoring. Journal of Air & Waste Management Association 51, 25–36.

Prospero, J.M., Savoie, D.L., 1989. Effect of continental sources on nitrate concentration over Pacific Ocean. Nature 339, 687.

Seinfeld, J.H., Pandis, S.N., 2006. Atmospheric Chemistry and Physics: From Air Pollution to Climate Change. John Wiley & Sons, Inc., New York.

Simon, P.K., Dasgupta, P.K., 1993. Wet effluent denuder coupled liquid ion chromatography systems–annular and parallel-plate denuders. Analytical Chemistry 65 (9), 1134–1139.

Simon, P.K., Dasgupta, P.K., 1995. Continuous automated measurement of gaseous nitrous and nitric-acids and particulate nitrite and nitrate. Environmental Science & Technology 29 (6), 1534–1541.

Slanina, J., ten Brink, H.M., Otjes, R.P., Even, A., Jongejan, P., Khlystov, A., Waijers-Ijpelaan, A., Hu, M., 2001. The continuous analysis of nitrate and ammonium in aerosols by the steam jet aerosol collector (SJAC): extension and validation of the methodology. Atmospheric Environment 35 (13), 2319–2330.

Sorooshian, A., Brechtel, F.J., Ma, Y.L., Weber, R.J., Corless, A., Flagan, R.C., Seinfeld, J.H., 2006. Modeling and characterization of a particle-into-liquid sampler (PILS). Aerosol Science and Technology 40 (6), 396–409.

Spicer, C.W., 1977. Photochemical atmospheric pollutants derived from nitrogen oxides. Atmospheric Environment 11, 1089–1095.

Spurny, K.R., 2000. Aerosol Chemical Processes in the Environment. Lewis.

Stelson, A.W., Seinfeld, J.H., 1982a. Relative humidity and temperature dependence of the ammonium nitrate dissociation constant. Atmospheric Environment 16 (5), 983–992.

Stelson, A.W., Seinfeld, J.H., 1982b. Thermodynamic prediction of the water activity, ammonium nitrate dissociation constant, density and refractive index for the ammonium nitrate-ammonium sulfate-water system at 25° C. Atmospheric Environment 16 (10), 2507–2514.

Stolzenburg, M.R., Hering, S.V., 2000. Method for the automated measurement of fine particle nitrate in the atmosphere. Environmental Science & Technology 34 (5), 907–914.

Sullivan, A.P., Weber, R.J., Clements, A.L., Turner, J.R., Bae, M.S., Schauer, J.J., 2004. A method for on-line measurement of water-soluble organic carbon in ambient aerosol particles: results from an urban site. Geophysical Research Letters 31 (13).

Sullivan, R.C., Guazzotti, S.A., Sodeman, D.A., Prather, K.A., 2006. Direct observations of the atmospheric processing of Asian mineral dust. Atmospheric Chemistry and Physics Discussions 6, 4109–4170.

Trebs, I., Meixner, F.X., Slanina, J., Otjes, R., Jongejan, P., Andreae, M.O., 2004. Real-time measurements of ammonia, acidic trace gases and water-soluble inorganic aerosol species at a rural site in the Amazon Basin. Atmospheric Chemistry and Physics 4, 967–987.

Umann, B., Arnold, F., Schaal, C., Hanke, M., Uecker, J., Aufmhoff, H., Balkanski, Y., Van Dingenen, R., 2005. Interaction of mineral dust with gas phase nitric acid and sulfur dioxide during the MINATROC II field campaign: first estimate of the uptake coefficient gamma(HNO_3) from atmospheric data. Journal of Geophysical Research-Atmospheres 110 (D22), D22306, doi:10.1029/2005JD005906.

Underwood, G.M., Song, C.H., Phadnis, M., Carmichael, G.R., Grassian, V.H., 2001. Heterogeneous reactions of NO_2 and HNO_3 on oxides and mineral dust: a combined laboratory and modeling study. Journal of Geophysical Research-Atmospheres 106 (D16), 18055–18066.

Weber, R., Orsini, D., Duan, Y., Baumann, K., Kiang, C.S., Chameides, W., Lee, Y.N., Brechtel, F., Klotz, P., Jongejan, P., ten Brink, H., Slanina, J., Boring, C.B., Genfa, Z., Dasgupta, P., Hering, S., Stolzenburg, M., Dutcher, D.D., Edgerton, E., Hartsell, B., Solomon, P., Tanner, R., 2003. Intercomparison of near real time monitors of $PM_{2.5}$ nitrate and sulfate at the US Environmental Protection Agency Atlanta Supersite. Journal of Geophysical Research-Atmospheres 108 (D7), 8421, doi:10.1029/2001JD001220.

Weber, R.J., Orsini, D., Daun, Y., Lee, Y.N., Klotz, P.J., Brechtel, F., 2001. A particle-into-liquid collector for rapid measurement of aerosol bulk chemical composition. Aerosol Science and Technology 35 (3), 718–727.

Wittig, A.E., Takahama, S., Khlystov, A.Y., Pandis, S.N., Hering, S., Kirby, B., Davidson, C., 2004. Semi-continuous $PM_{2.5}$ inorganic composition measurements during the Pittsburgh air quality study. Atmospheric Environment 38 (20), 3201–3213.

Xie, Y., Berkowitz, C.M., 2006. The use of positive matirx factorization with conditional probability functions in air quality studies: an application to hydrocarbon emissions in Huston, Texas. Atmospheric Environment 40, 3070–3091.

Yu, X.-Y., Lee, T., Ayres, B., Kreidenweis, S.M., Collett Jr., J.L., 2005. Particulate nitrate measurement using nylon filters. Journal of the Air & Waste Management Association 55, 1100–1110.

Yu, X.-Y., Lee, T., Ayres, B.R., Kreidenweis, S.M., Collett Jr., J.L., 2006. Loss of fine particle ammonium from denuded nylon filters. Atmospheric Environment 40, 4797–4807.

Zellweger, C., Ammann, M., Hofer, P., Baltensperger, U., 1999. NOy speciation with a combined wet effluent diffusion denuder-aerosol collector coupled to ion chromatography. Atmospheric Environment 33 (7), 1131–1140.

Zhuang, H., Chan, C.K., Fang, M., Wexler, A.S., 1999a. Formation of nitrate and non-sea-salt sulfate on coarse particles. Atmospheric Environment 33 (26), 4223–4233.

Zhuang, H., Chan, C.K., Fang, M., Wexler, A.S., 1999b. Size distributions of particulate sulfate, nitrate, and ammonium at a costal site in Hong Kong. Atmospheric Environment 33 (6), 843–853.